



# Thermal activation of kaolinite titanium hydroxide composite for uranium adsorption from aqueous solutions

M. S. Hagag<sup>1</sup> · Sh. M. A. Esmael<sup>1</sup> · F. Salem<sup>1</sup> · A. H. Ali<sup>1</sup> · S. A. Zaki<sup>1</sup>

Received: 17 June 2021 / Revised: 30 April 2022 / Accepted: 9 September 2022 / Published online: 3 October 2022  
© The Author(s) 2022

## Abstract

In the present study, thermally treated kaolinite at 600 °C was incorporated with titanium hydroxide produced from ilmenite to prepare a novel, low-cost and a promising adsorbent (KT). Different analytical techniques such as FTIR, EDS, SEM were used to determine its structural analysis. Its applicability for uranium uptake and desorption from its aqueous solutions was investigated by varying controlling conditions including pH, shaking time, initial concentrations, temperature and KT dose weight. Untreated kaolinite showed zero loading capacity and adsorption efficiency towards uranium ions, on the contrary thermal activation and incorporation with Ti(OH)<sub>4</sub> improved its performance. Batch results for adsorption experiments showed that loading capacity of (KT) reached 160 mg g<sup>-1</sup>; at pH 5, after only 20 min shaking time. Uranium adsorption process was much closer to a traditional Langmuir adsorption isotherm with a theoretical saturation capacity of 161.3 mg g<sup>-1</sup>. From thermodynamics data, the adsorption process is endothermic in nature which emphasized by elevating temperature has an enhancement effect on uranium adsorption with uptake of 205 mg g<sup>-1</sup> at 60 °C. Uranium adsorption was kinetically fitted with the pseudo-second-order model. KT composite has a high applicability and reusability due to its high resistance to extreme acidity levels.

**Keywords** Titanium hydroxide · Kaolinite · Adsorption isotherm · Uranium adsorption · Kinetics

## Introduction

Uranium is the most abundant and brilliant actinides element, represents the cornerstone of all nuclear industries whether peaceful or military, although its toxicity, radioactivity, and heavy metal pollution. Uranium resources are concentrated mainly in geological ores (e.g. uraninite, Carnotite, autunite), as well seawater. Uranium route from exploration sites to industrial uses passes via several stages to monitor and control environmental pollution. Whenever the dependency on nuclear power stations is intensifying, uranium explorations and separations increase as well. Many chemical techniques are designed for uranium separation and removal at the forefront, solvent extraction (Ali et al. 2018; Cheira 2020), adsorption (Morsy 2015; Feng et al. 2019;

Yousef et al. 2020a, b; Kouraim et al. 2020; Hagag 2020; Khani et al. 2006; Amesh et al. 2020; Hagag et al. 2022; Wang et al. 2015; Yousef et al. 2020a, b; Li et al. 2019 and Zhao et al. 2020), ion exchange resin (Aziz et al. 2010), inclusion membrane (and Zaheri 2020), liquid emulsion membrane (Sonali et al. 2018), and electroplating (Amoli et al. 2006). Exactly, solvent extraction and adsorption techniques are the most routinely used. In addition, the high uranium concentrations (> 1000 mg L<sup>-1</sup>) solvent extraction has the preference to be used economically and applicability at low acidic pH < 1 (Ali et al. 2018). Otherwise, the lower uranium concentrations (< 1000 mg L<sup>-1</sup>) adsorption is mostly carried out at high acidic pH or neutral (3–6) (Hagag 2020).

Generally, the most famous and abundance silicate clay minerals-kaolinite has chemical composition Al<sub>2</sub>Si<sub>2</sub>O<sub>5</sub>(OH)<sub>4</sub> that, occurred invariably in all continents (Kadir et al. 2014). The main uses of kaolinite cover many industrial areas inclusive but not limited to ceramics (Zeballos et al. 2016), cosmetics (Kamitsou et al. 2018), painting (Hradil et al. 2017) and cement (Bulanov et al. 2020). Indeed, scientifically main uses of kaolinite concentrated in adsorption studies (El-Maadawy 2019) and surpass cement and

---

Editorial responsibility: Samareh Mirkia.

✉ M. S. Hagag  
mohammedsobbhy@yahoo.com

<sup>1</sup> Nuclear Materials Authority, P.O. Box 530, Maadi, Cairo, Egypt



ceramics studies. Adsorption on kaolinite published in many works, for instance, low-cost adsorbent kaolinite (Mustapha et al. 2019), minerals surfaces protein-fragment (Awad et al. 2020),  $\text{PbCl}_2/\text{CdCl}_2$  (Li et al. 2021), pharmaceutical residues (Hounfodji et al. 2021) and composites doxycycline and Congo red (Sunday et al. 2020). Adsorption -the solid/liquid phase physio-chemical technique- day after day extensively growing up as a brilliant technique for removing heavy metals, pollutants, and valuable elements. Therefore it attracts scientific and industrial interests accordingly, its abundance of resources, low cost, applicability, and simplicity in preparation methods. Interestingly, wastes, ores, resins, zeolites, biomass, and composites originated as examples of adsorbents. Practically, to date, using the ores as adsorbents continuously broadcasted e.g. phosphate, kaolinite, granite, basalt, and muscovite.

In this work, the incorporation of highly purified  $\text{Ti}(\text{OH})_4$  originated from ilmenite with the thermally activated kaolinite produced KT composite, which has a crucial effect on enhancing adsorption efficiency and capacity towards uranium ions from aqueous solution with consideration of many cations of different valences. It is very significant to eliminate uranium from its containing samples e.g., nuclear fuel effluents tailings of the working mines, oceans and some industrial sources for its high radioactive effects besides, its toxicity hazards on the environment, surficial water and the groundwater. Eventually, the new adsorbent KT has many advantages including workability at low pH values, reusability, low cost of both raw materials, it is just possible that attaining positive eco-friendly and cost-effective aspects.

## Materials and methods

### Chemicals and methods

In this work, all used chemicals (salts or acids) were in the analytical grade, unless otherwise mentioned.  $\text{Ti}(\text{OH})_4$  was supplied by Black Sand project in Nuclear Materials Authority (NMA) thoroughly the extraction of ilmenite to be obtained with purity > 99.5%. In addition, kaolinite was supplied from NMA Geological Exploration sites. The working solutions were performed by mixing certain weights of salts with double distilled water DDW or deionized water DW.

### Composite preparation

KT composite was prepared via mixing 25gm of thermally activated kaolinite (at 600 °C) with 5gm of titanium hydroxide with a lesser amount of DDW. Eventually, the paste is shaken well until homogeneous slurry is formed. The former paste was heated at 110 °C for 2 h (until complete dryness)

and grinded in an agate mortar for producing a homogenous distribution of all composite ingredients.

### Adsorption and desorption studies

Batch experiments were carried out for uranium adsorption and desorption; in 50 mL transparent polyethylene tube the composite and the feeding solution were mixed and shaken in GLF water bath at room temperature unless otherwise stated. Generally, in pH studies, all extraction conditions were kept constant at (1000  $\text{mgL}^{-1}$  uranium concentration, 1 h equilibrium time, and 100 mg KT / 20 mL uranyl nitrate feeding solution), whereas, pH changed in range (1–6). Subsequently, initial uranium concentration changed in range (100–1000  $\text{mgL}^{-1}$ ), since the other extraction parameters were kept constant at pH 5, 1 h equilibrium time, and 100 mg KT / 20 mL uranyl nitrate feeding solution. Afterwards solid/liquid ratio studies were carried out at extraction parameters (pH 5, 1 h equilibrium time, and 1000  $\text{mgL}^{-1}$  uranium concentration). Thereafter, equilibrium time intervals are changed (5–60) min, and the other extraction parameters were fixed at (pH 5, 1 h equilibrium time, and 100 mg KT / 20 mL uranyl nitrate feeding solution and uranium concentration 1000  $\text{mgL}^{-1}$ ). Finally, the selectivity of KT was estimated via mixing individually standard solutions of  $\text{Th}^{4+}$ ,  $\text{Fe}^{3+}$ ,  $\text{Zn}^{2+}$ ,  $\text{Co}^{2+}$ ,  $\text{Al}^{3+}$ ,  $\text{SO}_4^{2-}$ , and  $\text{Cl}^-$  (1000  $\text{mgL}^{-1}$ ) to 1000  $\text{mgL}^{-1}$  uranyl nitrate solution at pH 5, 1 h equilibrium time, and 100 mg KT / 20 mL of uranyl nitrate feeding solution. Adsorption efficiency calculated from Eq. (1).

$$A\% = \frac{C_i - C_o}{C_i} \times 100 \quad (1)$$

A% is the adsorption efficiency and  $C_i$ ,  $C_o$ : are the initial and the remained uranium concentration after adsorption. Adsorbed uranium per unit mass of KT (adsorption capacity) is donated from the former Eq. (2).

$$q_e = \frac{C_i - C_o}{m} V \quad (2)$$

$q_e$  is the loading capacity of KT, V volume of uranium loading solution and m is the weight of KT adsorbent per mg.

### Uranium determination

Initially, both adsorption and elution residual (loaded KT) were discarded from working solution via Whatmann filter paper 52. Consequently, spectrophotometric determination was used for assaying the loaded and remained uranium via Arsenazo III method (Marczenko 1976). Moreover, the procedure concluded an aliquot of uranium solution (below concentration 1.5  $\text{mgL}^{-1}$ ), Arsenazo III 0.25%, urea-nitric solution, and ammonium hydroxide 25% the complexation

of uranium ions with Arsenazo III dye was measured at 650 nm with UV–VIS Shimadzu 1601 spectrophotometer. Ultimately, all pH measurements complemented with ion meter Orion 940 and Ross combination pH glass electrode. The Adjustments of pH for all adsorption experiments samples were executed with 0.1 N  $\text{HNO}_3$  and NaOH solutions.

## Results and discussion

### Characterization of KT composite

#### FT-IR spectroscopy

KT composite before and after uranium adsorption showed characteristic peaks on FT-IR charts related to different

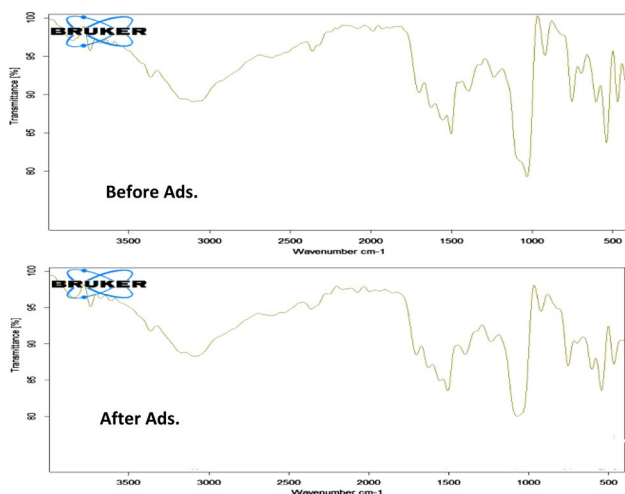


**Fig. 1** FTIR Spectra of KT composites before and after uranium adsorption

chemical bonds vibration or angel bending motion. Figure (1a before adsorption, b after adsorption) indicated FT-IR spectrum of KT composite before and after uranium adsorption. Generally, it showed bands at  $1090\text{ cm}^{-1}$  and  $460\text{ cm}^{-1}$  which represented stretching vibrational and angle bending of the bond Si—O—Si (Amesh et al. 2020). A bending motion appeared at  $563\text{ cm}^{-1}$  which outlined to Ti—O—H bond. The band at  $754\text{ cm}^{-1}$  represented Ti—O stretch (Wang and Andrews 2005). Finally, Fig. (1a, b) indicated that some bands are shifted to lower wavelengths and intensity after uranium adsorption on KT composite, as a result, may give evidence for uranium adsorption on KT.

### SEM charts of KT before and after uranium adsorption

SEM images in Fig. (2a before adsorption, b after adsorption) showed the surface morphology of KT composite and uranium-loaded KT. Generally, several grains size of agglomerated particles could be seen. In addition, a decrease in surface roughness obviously appears before and after uranium adsorption accompanying by an observable change in particle size and distribution. In the main time, after uranium adsorption some pores and crevices of KT composite are covered with uranium, as well the surface of composite became darker; furthermore, it may prove adsorption of uranium on KT surface.

### EDS charts for KT composite and uranium-loaded KT composite

Energy dispersive x-ray spectroscopy (EDS) for KT composite and uranium-loaded KT composite is shown in Fig. (3a before adsorption, b after adsorption). The major constituents of kaolinite were Al and Si, in addition to Fe, Ca, and K as minor constituents, which appear in Fig. (3a). Moreover, the peak of Ti was strongly present likewise, which represented the presence of  $\text{Ti}(\text{OH})_4$  peak in KT composite. Figure (3b) shows EDS chart of uranium-loaded KT composite, in addition, the presence of Ti, Al, and Si two peaks of uranium appeared, which may give qualitative proof for adsorption of uranium onto KT composite.

### Thermal activation of kaolinite

Adsorption efficiency and capacity of kaolinite for uranium ions are critically dependent on thermal activation. Actually the absence of thermal treatments is leading to zero adsorption efficiency and capacity of uranium on kaolinite minerals. Figure (4) indicating that increasing ignition temperature leads to activate the kaolinite surface for uranium adsorption. Hence, activation at temperatures 200, 300°C leads to uranium adsorption capacity of 4, 28 mg/g respectively. Eventually, uranium adsorption has maximal uptake of 31.25 mg/g at 600 °C, whereas, any increase in temperature is accompanied by stability in adsorption capacity and efficiency.

### Optimization of adsorption experiments

#### Effect of sample solution pH

Indeed, uranium ionic species in feeding solution depend basically on pH magnitude, hence reflect directly on both adsorption efficiency and capacity. The effect of pH change

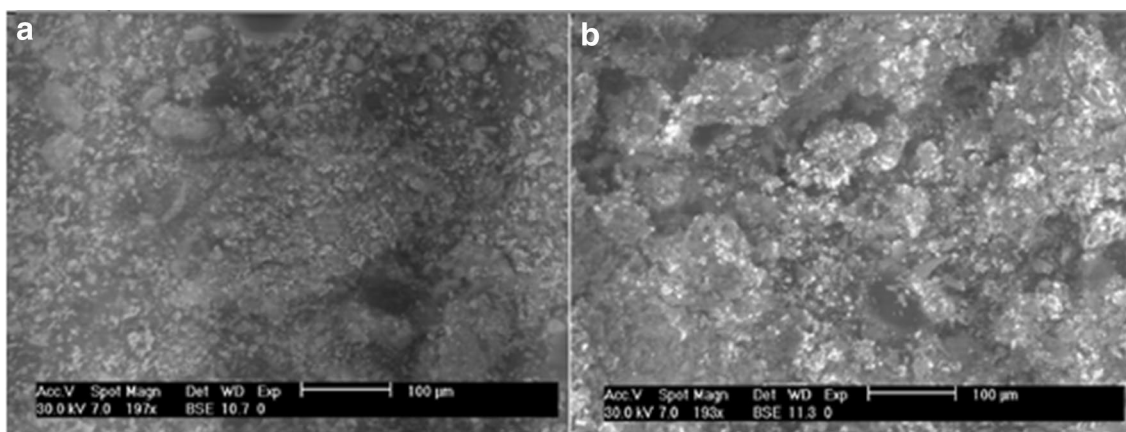


Fig. 2 a, b SEM images for KT composite before and after uranium adsorption

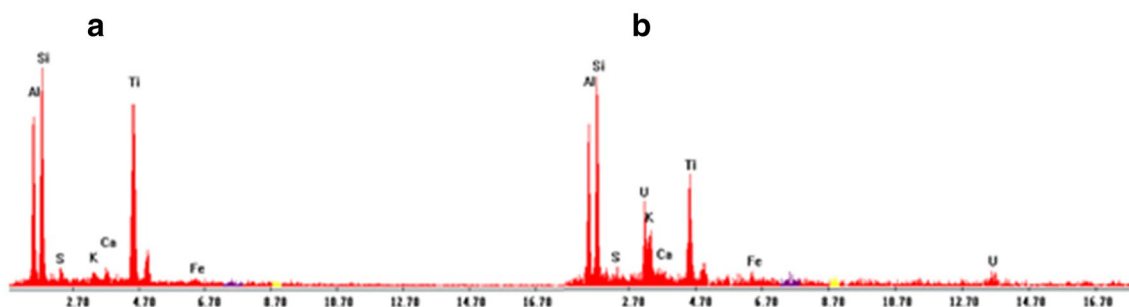
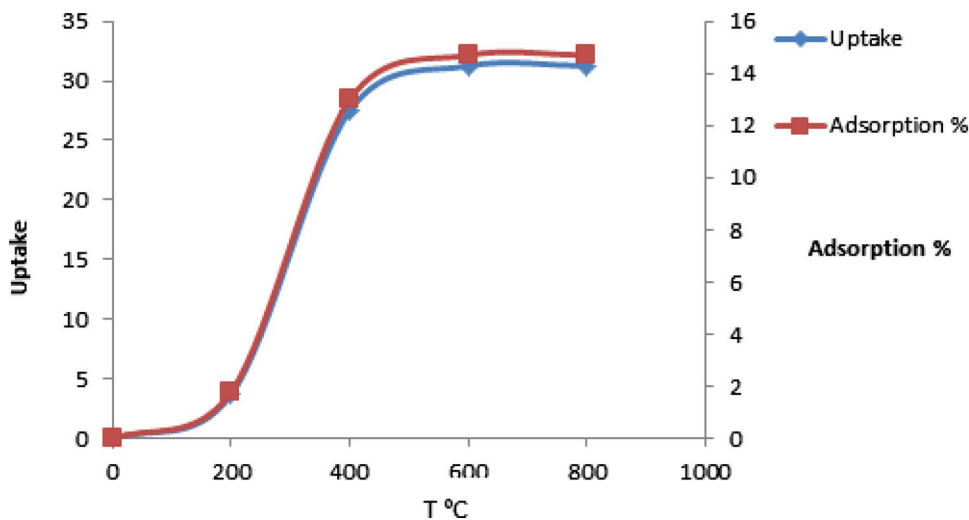


Fig. 3 a, b. EDS chart of KT composites before and after uranium adsorption

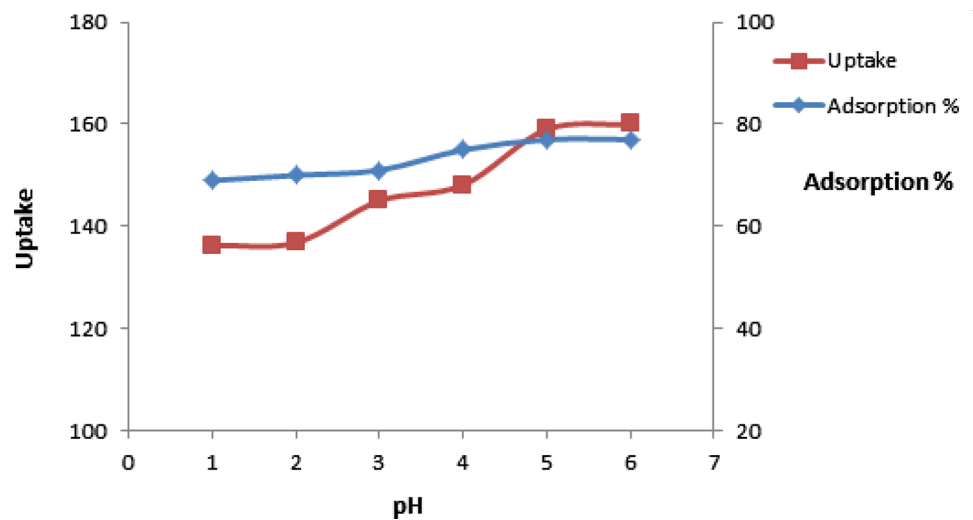
from (1–5) on adsorption is indicated in Fig. (5). Initially, changing pH in range (1–5) of uranium feeding solution has minimal effects on adsorption capacity which, diminished from 137 to 160 mg/g with ratio 16.5%. Therefore, KT composite adsorbed uranium despite pH change. Hence, at pH 5 the uranyl ion species were  $[\text{UO}_2\text{OH}]^+$ ,

$[(\text{UO}_2)_3(\text{OH})_4]^{2+}$ ,  $[(\text{UO}_2)_3(\text{OH})_5]^+$ ,  $[(\text{UO}_2)_2(\text{OH})_2]^{2+}$ ,  $[\text{UO}_2(\text{OH})_4]^{2-}$  and  $[(\text{UO}_2)_3(\text{OH})_7]^-$ ,  $[(\text{UO}_2)_2\text{OH}]^{3+}$ ,  $[(\text{UO}_2)_3(\text{OH})]^{5+}$ ,  $[(\text{UO}_2)_4(\text{OH})]^{7+}$  (Donia et al. (2009); Khani et al. 2006). Whereas, at  $\text{pH} > 5$  the negatively charged ionic uranium species existed, although the uranium adsorption uptake reached 160 mg/g. Eventually, at higher pH (6–8)

Fig. 4 effect of thermal activation for Kaolinite on uranium adsorption



**Fig. 5** effect of pH on uranium adsorption efficiency and uptake onto KT composite



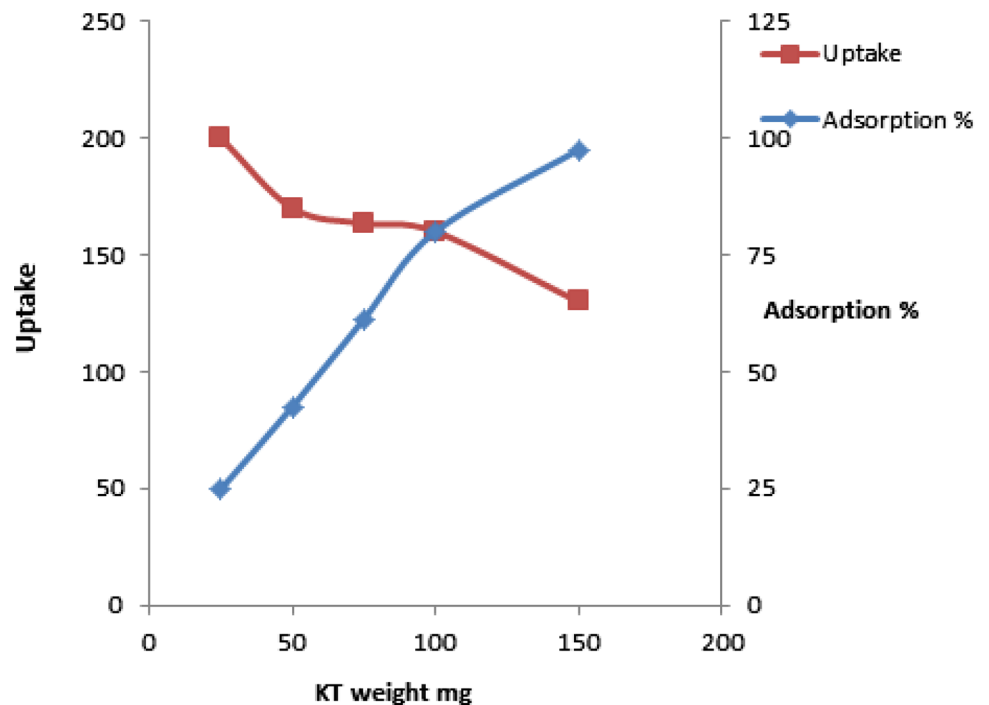
uranyl carbonate species  $(UO_2)_2(CO_3)(OH)^{3-}$  prevent adsorption, as well the adsorbent surface became negative, consequently adsorption efficiency and capacity decrease. Therefore, pH 5 is the optimum and is fixed in the subsequent adsorption experiments.

**Effect of dose weight on adsorption**

The effect of dosage weight of KT composite was identified by varying different weights in range (25–150) mg. As shown in Fig. (6) changing KT weights has a crucial role in values of adsorption efficiency ranging between (25–97.5)%, although, it is just possible that adsorption

capacity resemble behavior could be seen. Adsorption capacity has maximal value of  $200\text{mgg}^{-1}$  at KT weight 25 mg. Nevertheless, further increasing in KT weight from 50 to 150 mg could diminish adsorption capacity ( $170.2$  to  $130$ )  $\text{mgg}^{-1}$ . Since increasing KT weight with limiting uranium initial concentration ( $1000\text{mgL}^{-1}$ ) all uranium ions adsorbed but free active sites at KT are still unequipped; which conducted to decrease adsorption capacity at higher KT weights. KT weight of 0.1 mg is considered as an optimum for the subsequent adsorption experiments.

**Fig. 6** effect of KT weights on uranium adsorption and uptake



### Effect of uranium concentration

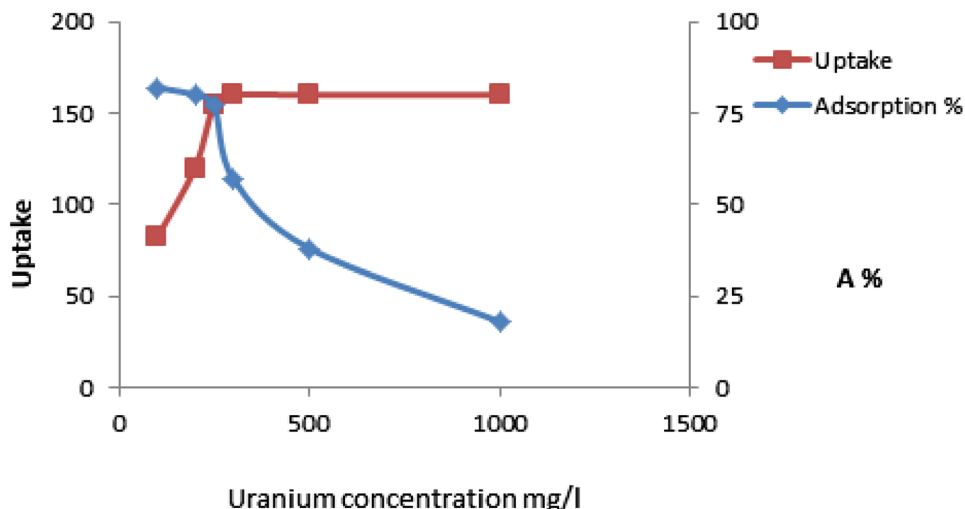
Generally, the effect of initial uranium concentration of the feeding solution was studied, as indicated in Fig. (7). The adsorption capacity of KT composite increased as uranium concentration increased from 100 to 250 mgL<sup>-1</sup> recording a significant increase from (82 to 160 mgg<sup>-1</sup>). Furthermore, increasing uranium concentration (100–250 mgL<sup>-1</sup>) per 100 mg KT weight, represented as consolidation for the driving force to diminish the mass transfer resistance between uranium in aqueous and surface of KT composite (Morsy 2015). Subsequently, at uranium concentrations > 250 mgL<sup>-1</sup>, the adsorption capacity reached maximum value owing to saturation KT surface with adsorbed uranyl ions. Unlike, adsorption efficiency showed different behavior than adsorption capacity. Consequently, it is just possible that the increase of uranium concentrations from 100 to 1000 mgL<sup>-1</sup> was accompanied by increasing values of adsorption

efficiency from 17 to 82% which may be attributed to the redundancy of existed uranyl ions with limitation of KT composite mass to 100 mg.

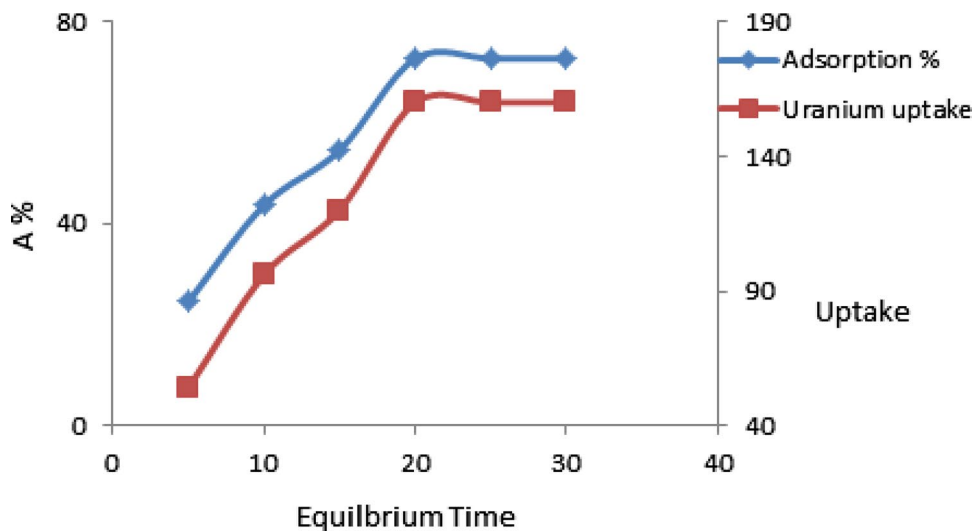
### Equilibrium time effect

The required time to achieve equilibrium uranium adsorption from aqueous phase to solid phase (active site at KT composite surface) was studied against adsorption capacity and efficiency as well, shown in Fig. (8). Moreover, providing data for kinetic studies at different temperature (25, 30, 40, 50, 60 °C) in kinetic models. Dynamic time was varied from (5–30 min) at 25 °C with adsorption capacity of KT composite. Interestingly, the uranium saturation capacity of adsorption attained 160mgg<sup>-1</sup> after only 20 min. Nevertheless, any increase in shaking time was accompanied by a steady loading capacity of 160mgg<sup>-1</sup>. Therefore, 20 min

**Fig. 7** effect of uranium concentration upon adsorption efficiency and uptake onto KT composite



**Fig. 8** Effect of contact time on adsorption and uptake of uranium onto KT composite



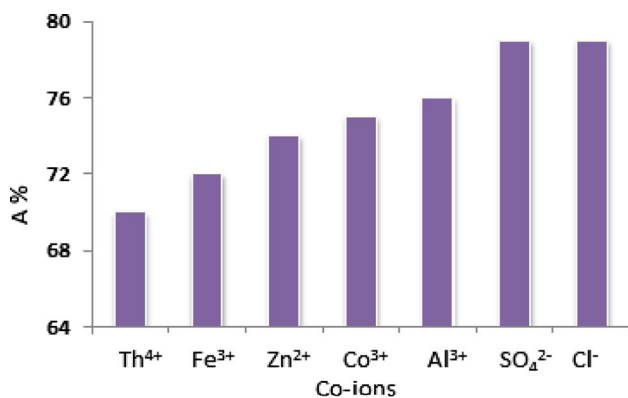


**Fig. 9** effect of Co-ions in uranium adsorption on KT composite

considered as optimum contact time and confirmed in the subsequent adsorption experiments.

### Selectivity of KT adsorbent for uranium ions

Selectivity of adsorbent is the centerpiece for determination the performance of adsorbent towards adsorbate ions. Generally, equal molar concentrations for different cations and anions were selected (Th<sup>4+</sup>, Fe<sup>3+</sup>, Co<sup>2+</sup>, Zn<sup>2+</sup>, Al<sup>3+</sup>, SO<sub>4</sub><sup>2-</sup> and Cl<sup>-</sup> 1000 mgL<sup>-1</sup>) and individually mixed with 1000 mg/l of uranyl ions for studying the co-ions effect on adsorption. Figure (9) revealed that KT composite having a good selectivity for uranyl ions in presence of these anions and cations. Whereas, Th<sup>4+</sup> ions caused 10% decrease in adsorption efficiency rather than other cations and anions gave about 5% (reduction in adsorption efficiency of uranium is established, i.e. adsorption efficiency reduced from 80 to 70% at 1000 mg/L of Th<sup>4+</sup>); which may be attributed to the high positive charge (4+) on thorium ions (Hagag et al 2020).

### Elution and regeneration studies

The uranium-loaded KT composite (after applying all optimum conditions of adsorption) was subjected to uranium desorption. Initially, different eluants were selected (NaCl, Na<sub>2</sub>CO<sub>3</sub>, HCl, H<sub>2</sub>SO<sub>4</sub>, HNO<sub>3</sub> 1 M and deionized water) for desorption whereas, other elution conditions are fixed (15 min contact time and 0.1 g/20 mL). Therefore, 1 M Na<sub>2</sub>CO<sub>3</sub> was sufficient to achieve > 99% desorption efficiency. Next, different concentrations of Na<sub>2</sub>CO<sub>3</sub> (0.25–1 M) were shaken with 0.1 g/20 mL of loaded KT at 15 min. The optimum concentration of Na<sub>2</sub>CO<sub>3</sub> was 0.75 M since it achieved 99.5% desorption efficiency. Eventually, 15 min was the optimum contact time after shaking different interval times (5–20 min) with 20 mL of Na<sub>2</sub>CO<sub>3</sub> and 100 mg of uranium-loaded KT composite. Figures (10, 11, 12) show the elution efficiency versus eluants type, eluant

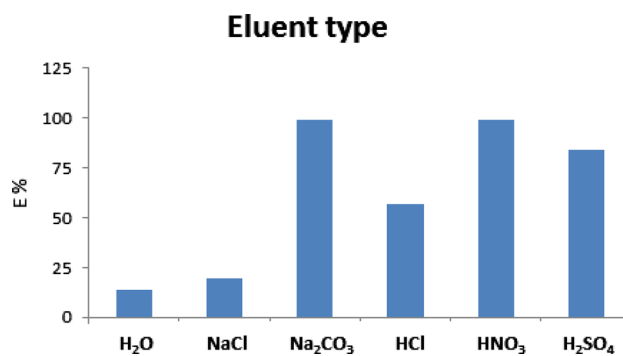


**Fig. 10** effect of eluent type on uranium desorbing efficiency from loaded KT

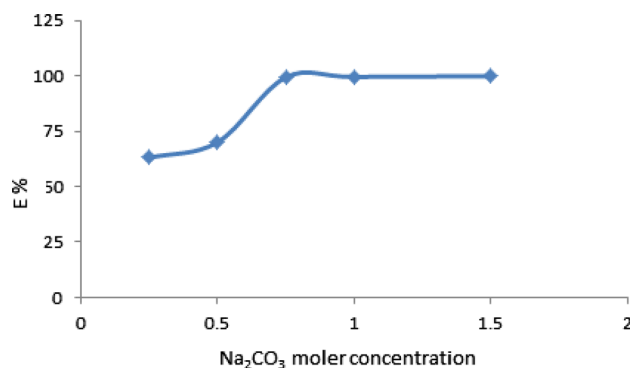


**Fig. 11** effect of Na<sub>2</sub>CO<sub>3</sub> concentration on uranium desorbing efficiency from loaded KT

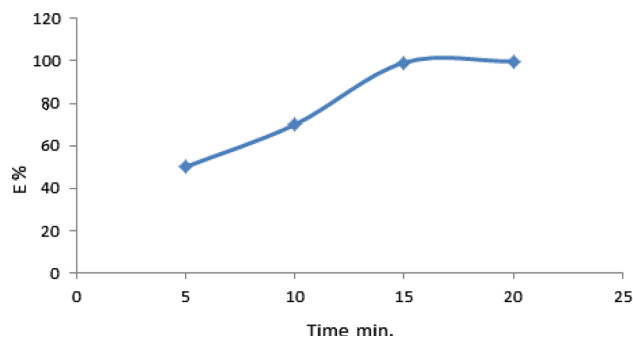


**Fig. 12** effect of contact time on uranium desorbing efficiency from loaded KT composite

concentration, and contact time respectively. Finally, the KT composite showed high resistance to acidic attack at lower pH as well, high temperature.

### Effect of temperature on adsorption

Unlike, the stated in many papers (increasing temperature negatively affected both adsorption efficiency and capacity) whereas, uranium adsorption on KT adsorbent enhanced



and accelerated by rising temperature. Adsorption at different temperatures (25 (room temperature)—30, 40, 50, 60 °C) was studied under constant volume 20 ml, 100 mg KT, 20 min contact time and 1000 mgL<sup>-1</sup> uranium concentration. Accordingly, the positive effect of rising temperature on adsorption is attributed to the chemisorption nature of uranium adsorption on KT composite. Figure (13) revealed that at 25–30 °C the uranium uptake was nearly constant at 160mgg<sup>-1</sup>. Nevertheless, rising temperature (40, 50, 60 °C) reflected positively on increasing uranium uptake of (170–180–205 mgg<sup>-1</sup>) respectively, as a result of activation energy for chemisorption of uranium at KT composite. Similarly, The effect of elevation temperature (30, 40, 50, 60 °C) on dynamic time-adsorption capacity curves showed a resemble behavior to 25 °C.

### Adsorption isotherm studies

Adsorption isotherm gives a descriptive interpretation for uranium transportation from aqueous media to the solid-phase surface of KT composite. Although many models of adsorption isotherm have been used, Langmuir and Freundlich are the most commonly, applicable, and extensively used models. Langmuir isotherm model gives a conception to form uniformly uranyl ion adsorption on KT surface via formation of homogeneous monolayer over finite degenerated active sites at the composite surface. Equation (3) represented mathematical Langmuir model (Langmuir 1916; Bhatti and Hamid 2014; Hagag et al 2020):

$$\frac{C_e}{q_e} = \frac{1}{bq_0} + \frac{C_e}{q_0} \quad (3)$$

Where  $q_0$  is the maximum theoretical uptake of KT composite mgg<sup>-1</sup>,  $b$  is the Langmuir equilibrium constant l/mg

**Fig. 13** effect of temperature on uranium adsorption efficiency and uptake onto KT composite

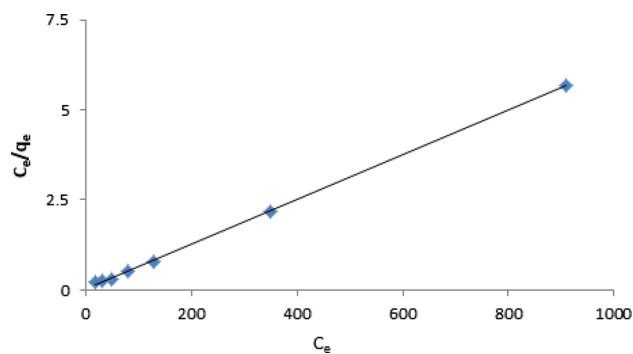
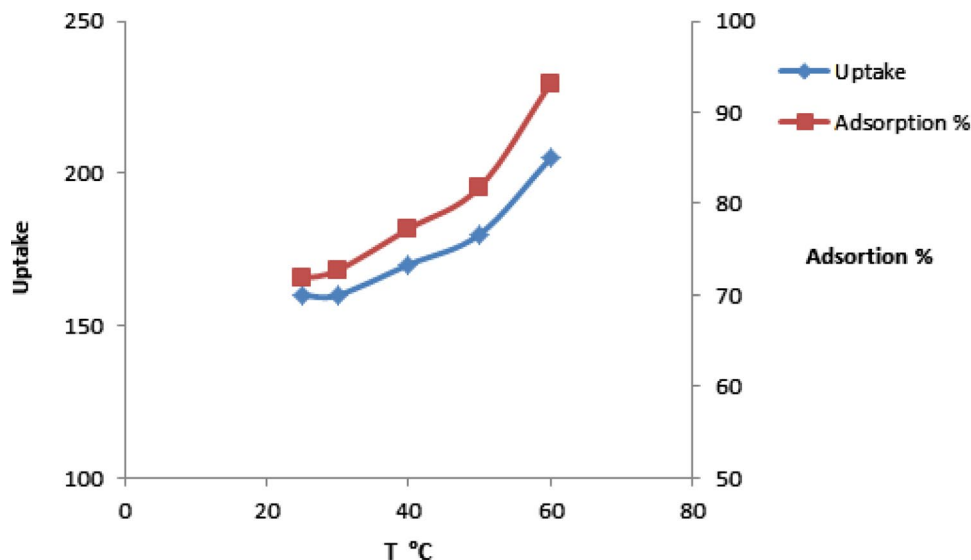


**Fig. 14** Langmuir isotherm graph for adsorption of uranium on KT composite

measuring adsorption energy (Fig. 14) shown the Langmuir model of uranyl ion adsorption on KT composite, moreover, the value of  $q_0$  and  $K$  designated from slope and intercept. Freundlich isotherm model unlike, Langmuir model which stated that active site on the adsorbent surface is degeneratedly distributed, the term of heterogenic active site distribution over adsorbate surface predominated in Freundlich model. In addition, multi-layers of adsorbate ions adsorbed over adsorbent surfaces were formed. Equation (4) represented mathematical formula for Freundlich model (Freundlich 1906; Zhang et al. 2022; Hagag et al 2020; Kouraim and Hagag 2020).

$$\log q_e = \log K_F + \frac{1}{n} \log C_e \quad (4)$$

where:  $K_f$  and  $n$  parameters are theoretical adsorption capacity of KT and dimensionless Freundlich constant related to adsorption heterogeneity respectively. Figure (15) indicated Freundlich isotherm model for uranium adsorption, furthermore, the value of  $q_0$  and  $K$  designated from slope and



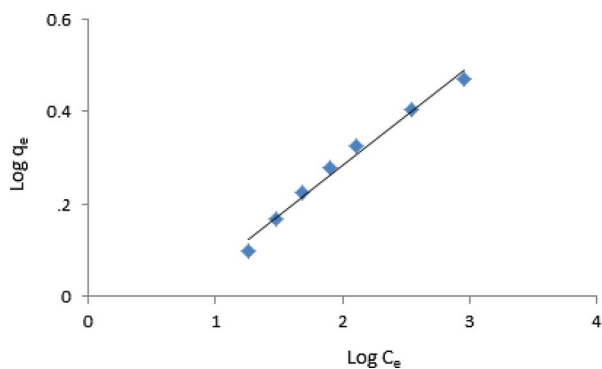


**Fig. 15** Freundlich isotherm graph for adsorption of uranium on KT composite

intercept values. Indeed, the value of correlation coefficient  $R^2$ , constants, and maximum theoretical adsorption capacity  $q_0$  for Langmuir and Freundlich models were obtained in table (1). The uranium adsorption dependency on Langmuir or Freundlich isotherm model was determined via  $q_0$  and  $R^2$  values of the two models. Accordingly, Langmuir model exhibited  $R^2$  (0.9994) much closer to unity, in addition, theoretical adsorption capacity value of ( $161.5 \text{ mg g}^{-1}$ ) was much closer to practical uptake. Contradictory, Freundlich model exhibited  $R^2$  (0.987) lesser than Langmuir model, as well as a poorly fitted theoretical loading capacity of ( $6.11$ ) compared with practical uptake ( $160 \text{ mg g}^{-1}$ ). Eventually, uranium adsorption on KT composite was in accordance with Langmuir isotherm model.

The Dubinin–Radushkevich model implied that loading capacity related to the amount of the adsorbate (uranium) that is being adsorbed on the adsorbent (KT composite), unlike the Langmuir isotherm model. The mathematical equation of Dubinin–Radushkevich is symbolized by Eq. (5):

$$\ln q_e = \ln q_m - K\epsilon^2 \tag{5}$$

where:  $q_e$ : the amount of uranium adsorbed per unit mass of KT composite ( $\text{mg g}^{-1}$ ),  $q_m$ : defined as the theoretical loading capacity for uranium ( $\text{mg g}^{-1}$ ),  $K$ : is defined as a constant related to the adsorption energy ( $\text{mol}^2 \text{ kJ}^{-2}$ ),  $\epsilon$ : is defined as the adsorption potential ( $\text{kJ mol}^{-1}$ ) and is calculated from equation  $\epsilon = RT \ln (1 + 1/C_e)$  (Youssef et al. 2018). The main advantage of the Dubinin–Radushkevich model is the determination of adsorption energy  $E$  depending on  $K$  (constant of the adsorption energy) value, where  $E = 1/(2 K)^{1/2}$ . Accordingly, the adsorption type (chemisorption

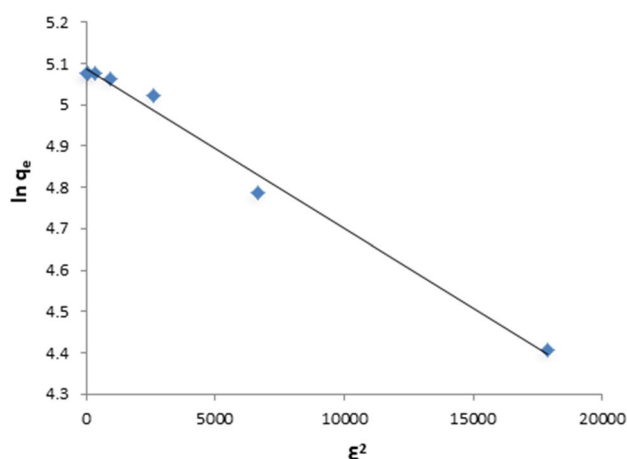


**Fig. 16** Dubinin–Radushkevich isotherm graph for adsorption of uranium on KT composite

or physisorption) is determined depending on  $E$  value, generally, if  $E$  value is lower than 8 actually the adsorption process is physisorption, inversely to that if the value is greater than 8 then the adsorption process is chemisorption. The Dubinin–Radushkevich model curve is shown in Fig. (16) X-axis represented  $\epsilon^2$  and Y-axis represented  $\ln q_e$ . Slope calculations outlined that the exact value of adsorption energy is  $113.9 \text{ J mol}^{-1}$ , greater than 8 which supported that uranium adsorption over KT composite is chemisorption,  $q_m$ , that is being displayed through the intercept value is about  $161.8 \text{ mg g}^{-1}$ , which was in accordance with practical loading capacity of uranium over KT composite.

**Kinetic models of adsorption**

Kinetic models described dynamicity of the adsorption process and included many models, for and foremost Pseudo-first-order model and Pseudo-second-order model are the most commonly employed models. Indeed, Pseudo-first-order kinetic model was a bimolecular reaction in nature but depends greatly on one reactant rather than the other; therefore adsorption was closer to physisorption process. Lagergren equation Eq. (6) was a mathematical description for Pseudo-first-order model (Lagergren 1898; Broujeni et al. 2019; Hagag 2020).

$$\log(q_e - q_t) = \log q_e - \left( \frac{k_1}{2.303} \right) t \tag{6}$$

**Table 1** Langmuir and Freundlich parameters and constants for uranium adsorption onto KT composite

| Composite | Langmuir model parameters |            |        | Freundlich model parameters |       |        |
|-----------|---------------------------|------------|--------|-----------------------------|-------|--------|
|           | $q_0$ (mg/g)              | $b$ (L/mg) | $R^2$  | $K_f$                       | $1/n$ | $R^2$  |
| KT        | 161.3                     | 0.152      | 0.9994 | 0.713                       | 0.21  | 0.9877 |

**Fig. 17** pseudo-first- order model at (25, 30,40,50,60 °C) for uranium adsorption onto KT composite

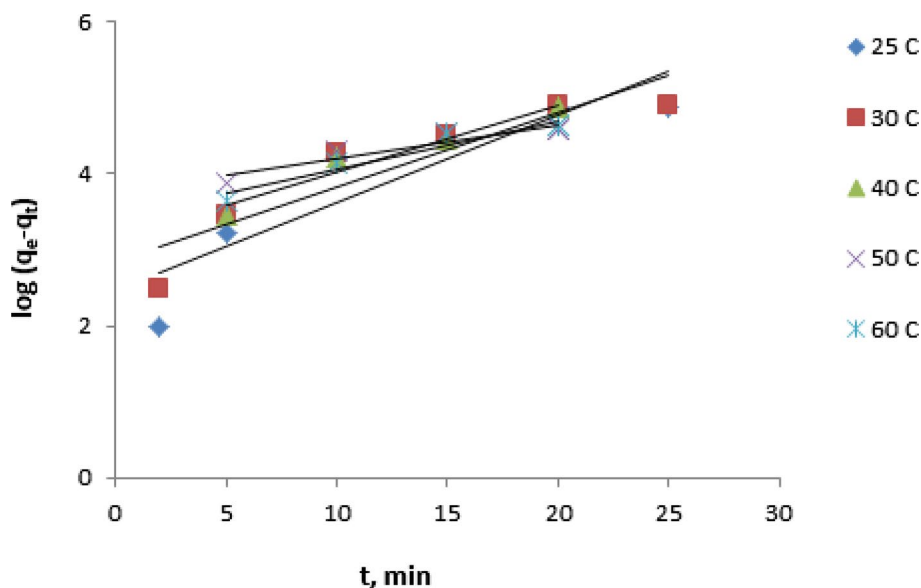


**Table 2** Pseudo first and second-order kinetic models constants for of uranium adsorption on KT composite

| KT composite | The pseudo-first-order kinetic model |        |       | The pseudo-second-order kinetic model |                      |       |
|--------------|--------------------------------------|--------|-------|---------------------------------------|----------------------|-------|
|              | $q_e$ (mg/g)                         | $K_1$  | $R^2$ | $q_e$                                 | $K_2$                | $R^2$ |
|              | 30                                   | 0.0032 | 0.933 | 139.2                                 | $8.4 \times 10^{-4}$ | 0.978 |

where,  $q_t$  is the mass of uranium adsorbed on KT composite at time  $\text{mg/g}^{-1}$ ,  $K_1$  pseudo first order constant  $\text{min}^{-1}$ . Generally, Fig. (17) represented the plotting of  $\text{Log}(q_e - q_t)$  versus  $t$  and determined the theoretical equilibrium saturation capacity  $q_e$  and order constant at 25 °C from slope and intercept thereby, mentioned in table (2), therefore on the basis of  $R^2$ ,  $q_e$  values of 0.933 and  $30 \text{ mgg}^{-1}$  respectively, dynamic uranium adsorption on KT was still out of accordance with Pseudo-first-order model.

Pseudo-second-order model was a bimolecular reaction, greatly depending on concentration of uranium and KT composite. Hence, it was commonly much closer to chemisorption process. Pseudo-second-order model was described mathematically by Eq. (7) (Kumar and Sivanesan 2006; Broujeni et al. 2019; Hagag 2020):

$$\frac{t}{q_t} = \frac{1}{K_2 q_e^2} + \left(\frac{1}{q_e}\right)t \tag{7}$$

where:  $K_2$  Pseudo-second-order rate constant ( $\text{g mg}^{-1} \text{ min}^{-1}$ ), plotting  $t/q_t$  against  $t$  was shown in Fig. (18). Next the values of  $R^2$  and  $q_t$  were 0.978 and  $139.2 \text{ mgg}^{-1}$  respectively at 25 °C, (calculated from the slope and intercept). Eventually, Table (2) showed correlation coefficients, rate constants and adsorption capacities for both models. Consequently, values of  $R^2$  and  $q_e$ , for pseudo-first and pseudo-second-order models were 0.933, 0.978,  $30 \text{ mgg}^{-1}$

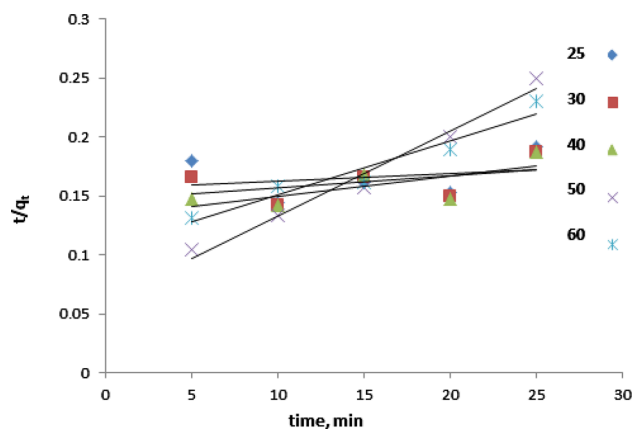


**Fig. 18** pseudo-second- order model at (25,30,40,50,60 °C) for uranium adsorption onto KT composite

$139.2 \text{ mgg}^{-1}$  respectively, indicated that uranium adsorption on KT surface dynamically corresponded to Pseudo-second-order model. Notably, elevated temperatures (30, 40, 50, 60 °C) enhanced uranium chemisorption on KT as well, increased uptake ( $160, 170, 180, 205 \text{ mgg}^{-1}$ ) respectively as former stated. Figures (17, 18) showed the effect of temperature in Pseudo-first-order and Pseudo-second-order models. Similarly, The effect of elevated temperature (30, 40, 50, 60 °C) on Pseudo-first-order and Pseudo-second-order models showed a resemble behavior at 25 °C i.e. uranium adsorption

over KT composite fitted with Pseudo-second-order model at higher temperature.

## Conclusion

Thermal activation of kaolinite and also incorporation with  $\text{Ti}(\text{OH})_4$  improved its loading capacity towards uranium from zero to  $160 \text{ mgg}^{-1}$  at maximum optimal extraction conditions (100 mg of KT composite/ 20 mL of  $1000 \text{ mgL}^{-1}$  of uranyl nitrate, pH 5 and 20 min dynamic equilibrium time). The optimum desorption conditions were 100 mg of uranium-loaded KT composite/ 20 mL of 0.75 M  $\text{Na}_2\text{CO}_3$  and 15 min contact time. Uranium adsorption over KT composite was much closer to be in accordance with Langmuir adsorption model with  $R^2$  and theoretical capacity values ( $161.5 \text{ mgg}^{-1}$ , 0.9994) rather than Freundlich isotherm model. In addition, the adsorption was fitted with kinetic-pseudo second order-model and this fitting continued to higher temperature (30, 40, 50, 60 °C). The adsorption of uranium on KT adsorbent was chemisorbed, hence positively enhanced with rising temperature, thus 60 °C giving uranium uptake over KT adsorbent  $205 \text{ mgg}^{-1}$ .

**Acknowledgments** The authors wish to thank all who assisted in conducting this work.

**Author contributions** All authors contributed to the study conception and design, Material preparation, data collection and analysis. All authors read and approved the final manuscript.

**Funding** Open access funding provided by The Science, Technology & Innovation Funding Authority (STDF) in cooperation with The Egyptian Knowledge Bank (EKB). The authors received no financial support for the research, authorship, and/or publication of this article.

**Availability of data and materials** All the data used for this work are publicly available.

## Declarations

**Conflict of interest** All authors declare that they have no conflict of interest.

**Competing interest** All authors declare competing interests.

**Consent to participate** All of the authors consented to participate in the drafting of this manuscript.

**Consent for publication** All of the authors consent to publish this manuscript.

## Ethical approval

All authors confirm that the manuscript has been read and approved. All authors declare that this manuscript has not been published and not under consideration for publication elsewhere.

**Open Access** This article is licensed under a Creative Commons Attribution 4.0 International License, which permits use, sharing, adaptation, distribution and reproduction in any medium or format, as long as you give appropriate credit to the original author(s) and the source, provide a link to the Creative Commons licence, and indicate if changes were made. The images or other third party material in this article are included in the article's Creative Commons licence, unless indicated otherwise in a credit line to the material. If material is not included in the article's Creative Commons licence and your intended use is not permitted by statutory regulation or exceeds the permitted use, you will need to obtain permission directly from the copyright holder. To view a copy of this licence, visit <http://creativecommons.org/licenses/by/4.0/>.

## References

- Ali AH, Atef A, Hagag MS (2018) Upgrading of the crude yellowcake to a highly purified form using tris(2-ethylhexyl) phosphate in presence of EDTA or CDTA. *J Env Chem Eng* 7(1):117–129. <https://doi.org/10.1016/j.jece.2017.11.07>
- Amesh P, Suneesh AS, Venkatesan KA, Chandra M, Ravindranath NA (2020) High capacity amidic succinic acid functionalized mesoporous silica for the adsorption of uranium. *Colloid Surf Physicochem Eng Aspects*. <https://doi.org/10.1016/j.colsurfa.2020.125053>
- Amoli HS, Barker J, Flowers A (2006) Electrodeposition and determination of nano-scale uranium and plutonium using alpha-spectroscopy. *J Radioanal Nucl Chem*. <https://doi.org/10.1007/s10967-006-0197-3>
- Awad ME, Borrego-Sanchez A, Escamilla-Roa E, Hernandez-Laguna A, Sainz-Diaz CI (2020) Modeling of the adsorption of a protein-fragment on kaolinite with potential antiviral activity. *Appl Clay Sci* 199:105865. <https://doi.org/10.1016/j.clay.2020.105865>
- Aziz A, Jan S, Waqar F (2010) Selective ion exchange separation of uranium from concomitant impurities in uranium materials and subsequent determination of the impurities by ICP-OES. *J Radioanal Nucl Chem* 284:117–121
- Bhatti HN, Hamid S (2014) Removal of uranium(VI) from aqueous solutions using eucalyptus citriodora distillation sludge. *Int J Environ Sci Technol* 11:813–822. <https://doi.org/10.1007/s13762-013-0267-3>
- Broujeni BRN, A, Hassani AH, Saberi R, (2019) Comparative adsorption study of  $\text{Th}^{4+}$  from aqueous solution by hydrothermally synthesized iron and aluminum oxide nanoparticles. *Int J Environ Sci Technol*. <https://doi.org/10.1007/s13762-018-1824-6>
- Bulanov PE, Ermilova EY, Rakhimov RZ (2020) Structure and mineral composition of soil cement based on kaolinite clay modified with a complex hydrophobic-plasticizer additive based on polycarboxylate ether and octyltriethoxysilane. *Polym Sci Ser D* 13:447–452. <https://doi.org/10.1134/S199542122004005X>
- Cheira MF (2020) Solvent extraction of uranium and vanadium from carbonate leach solutions of ferruginous siltstone using cetylpyridinium carbonate in kerosene. *Chem Pap* 74:2247–2266. <https://doi.org/10.1007/s11696-020-01073-w>
- Donia AM, Atia AA, Moussa EMM, El-Sherif AM, El-Magied AO A (2009) Removal of uranium(VI) from aqueous solutions using glycidyl methacrylate chelating resins. *Hydrometallurgy* 95(3–4):183–189. <https://doi.org/10.1016/j.hydromet.2008.05.037>
- El-Maadawy MM (2019) HDEHP-impregnated kaolinite for adsorption of uranium from dilute phosphoric acid. *Radiochemistry* 61:331–338. <https://doi.org/10.1134/S1066362219030081>



- Feng Y, Ma B, Guo X (2019) Preparation of amino-modified hydroxyapatite and its uranium adsorption properties. *J Radioanal Nucl Chem* 319:437–446. <https://doi.org/10.1007/s10967-018-6357-4>
- Freundlich MF (1906) Über die adsorption in lasungen. *Z Phys Chem* 57:385–470
- Hagag MSA (2020) Comparative study of fabricated composites based on phosphogypsum and Al-hydroxide for uranium separation from aqueous and waste solutions. *Int J Environ Anal Chem* 101(5):680–701. <https://doi.org/10.1080/03067319.2019.1670826>
- Hagag MS, Morsy AMA, Ali AH (2020) Adsorption of rare earth elements onto the phosphogypsum a waste byproduct. *Water Air Soil Pollut* 230:308. <https://doi.org/10.1007/s11270-019-4362-z>
- Hagag MS, Esmaeel SM, Salem F, Zaki SA, and Ali AH, (2022) Uranium sorption from waste solutions by Talc Phosphogypsum ferri-Uranium sorption from waste solutions by Talc Phosphogypsum ferri- silicate synthetic new sorbent" *Radiochimica Acta*, 110 (2) : 93–106. <https://doi.org/10.1515/ract-2021-1061>
- Hounfodji JW, Kanhounon WK, Kpotin G, Atohoun GS, Lainé J, Foucaud Y (2021) Badawi M (2021) Molecular insights on the adsorption of some pharmaceutical residues from wastewater on kaolinite surfaces. *Chem Eng J* 407:1385–8947. <https://doi.org/10.1016/j.cej.2020.127176>
- Hradil D, Hradilov J, Bezdika P, Matulkov I (2017) Kaolinite-alunite association in late Gothic white grounds from Slovakia: a local peculiarity in painting technology. *Appl Clay Sci* 144:79–87. <https://doi.org/10.1016/j.clay.2017.05.004>
- Kadir S, Kùlah T, Eren M (2014) Mineralogical and geochemical characteristics and genesis of the gùlzelyurtalunite-bearing kaolinite deposit within the late miocene godeles ignimbrite, Central Anatolia. *Turkey Clays Clay Miner* 62:477–499. <https://doi.org/10.1346/CCMN.2014.0620603>
- Kamitsou MD, Sygouni V, Kanelloupolou DG (2018) Physicochemical characterization of sterilized muds for pharmaceuticals/cosmetics applications. *Environ Geochem Health* 40:1449–1464. <https://doi.org/10.1007/s10653-017-0066-8>
- Khani MH, Keshtkar AR, Meysami B, Zarea MF, Jalali R (2006) Biosorption of uranium from aqueous solutions by nonliving biomass of marinealgae cystoseira. *Electronic J Biotechnol* 9:101–106. <https://doi.org/10.2225/vol9-issue2-fulltext-8>
- Kouraim MN, Hagag MS & Ali AH. (2020) Sorption of uranium from radioactive wastes by silicate-neutralised polyacrylic. *Int J Environ Anal Chem* 100(7):825–840. <https://doi.org/10.1080/03067319.2019.1641600>
- Kouraim MN, Hagag MS, Ali AH (2020) Adsorption of uranium from its aqueous solutions using activated cellulose and silica grafted cellulose. *Radiochim Acta* 108(4):261–271. <https://doi.org/10.1515/ract-2019-3149>
- Kumar KV, Sivanesan S (2006) Pseudo second order kinetics and pseudo isotherms for malachite green onto activated carbon: comparison of linear and non-linear regression methods. *J Hazard Mater* 136(3):721–726
- Lagergren S (1898) Zur Theorie der sogenannten adsorption gelosterstoffe. *K Sevn Vetenskapsakad Handl* 24:1–39
- Langmuir, (1916) The constitution and fundamental properties of solids and liquids. *J Am Chem Soc* 38:2221–2295
- Li L, Hu N, Dai Z, Lu W (2019) Efficient and selective removal of uranium(VI) from aqueous solution by ethylenediamine- and amidoxime-decorated *Aspergillus niger*. *Int J Environ Sci Technol* 16:7523–7534. <https://doi.org/10.1007/s13762-018-2154-4>
- Li J, Zhong Z, Du H, Li Q, Wang N, Zhao H, Huang J (2021) Theoretical study on the adsorption mechanism of PbCl<sub>2</sub>/CdCl<sub>2</sub> by kaolinite during municipal solid waste pyrolysis. *Chemosphere* 267:29184. <https://doi.org/10.1016/j.chemosphere.2020.129184>
- Marczenko Z (1976) Spectrophotometric determination of elements. Halsted Press, New York
- Morsy AM (2015) Adsorptive removal of uranium ions from liquid waste solutions by phosphorylated chitosan. *Environ Technol Innov* 4:299–310. <https://doi.org/10.1016/j.eti.2015.10.002>
- Mustapha SN, damitso MM, Abdulkareem AS, Tijani JO, Mohammed AK, Shuaib DT, (2019) Potential of using kaolin as a natural adsorbent for the removal of pollutants from tannery wastewater. *Heliyon* 5(11):e02923. <https://doi.org/10.1016/j.heliyon.2019.e02923>
- Sonali SK, Vinay AJ, Mukhopadhyay S (2018) Intensification of emulsion liquid membrane extraction of uranium(VI) by replacing nitric acid with sodium nitrate solution. *Chem Eng Proc Process Intensification* 125:18–26. <https://doi.org/10.1016/j.cep.2017.12.021>
- Sunday J, Olusegun SJ, Mohallem NDS (2020) Comparative adsorption mechanism of doxycycline and Congo red using synthesized kaolinite supported CoFe<sub>2</sub>O<sub>4</sub> nanoparticles. *Environ Pollut* 260:114019. <https://doi.org/10.1016/j.envpol.2020.114019>
- Uranium sorption from waste solutions by Talc Phosphogypsum ferri- silicate synthetic new sorbent" *Radiochimica Acta* 110 (2) : 93–106. <https://doi.org/10.1515/ract-2021-1061>
- Wang X, Andrews L (2005) *J Phys Chem A* 109(47):10689–10701. <https://doi.org/10.1021/jp054482i>
- Wang YD, Li GY, Ding DX (2015) Column leaching of uranium ore with fungal metabolic products and uranium recovery by ion exchange. *J RadioanalNuclChem* 304:1139–1144. <https://doi.org/10.1007/s10967-015-3957-0>
- Yousef LA, Bakry AR, Ahmad AA (2020a) Uranium(VI) adsorption using a mixture of 1-amino-2-naphthol-4-sulfonic acid and bentonite: kinetic and equilibrium studies. *Radiochemistry* 62:769. <https://doi.org/10.1134/S1066362220060090>
- Yousef LA, Morsy AMA, Hagag MS (2020b) Uranium ions adsorption from acid leach liquor using acid cured phosphate rock: kinetic, equilibrium, and thermodynamic studies. *Sep Sci Technol* 55(4):648–657. <https://doi.org/10.1080/01496395.2019.157430>
- Youssef WM, Hagag MS, Ali AH (2018) Synthesis, characterization and application of composite derived from rice husk ash with aluminium oxide for sorption of uranium. *Adsorpt Sci Technol* 36(5–6):1274–1293. <https://doi.org/10.1177/0263617418768920>
- Zaheri P, Davarkhah R (2020) Selective separation of uranium from sulfuric acid media using a polymer inclusion membrane containing alamine336. *Chem Pap*. <https://doi.org/10.1007/s11696-019-01029-9>
- Zeballos A, Weihed P, Blanco M (2016) Geological, mineralogical and chemical characterization of Devonian kaolinite-bearing sediments for further applications in the ceramic (tiles) industry in La Paz. *Bolivia Environ Earth Sci* 75:546. <https://doi.org/10.1007/s12665-015-5212-y>
- Zhang L, Chen Y, Zhao M, Wang YH (2022) Efficient adsorption of uranyl ions from aqueous solution by Gd<sub>2</sub>O<sub>3</sub> and Gd<sub>2</sub>O<sub>3</sub>-MgO composite materials. *Int J Environ Sci Technol*. <https://doi.org/10.1007/s13762-022-04001-5>
- Zhao D, Yang S, Chen S (2020) Correction to: effect of pH, ionic strength and humic substances on the adsorption of Uranium (VI) onto Na-rectorite. *J RadioanalNuclChem* 323:1013. <https://doi.org/10.1007/s10967-019-06994-9>